Stochastic resonance as a crisis in a period-doubled circuit

T. L. Carroll and L. M. Pecora
Naval Research Laboratory, Washington, D.C. 20375
(Received 12 February 1993)

Stochastic resonance, a phenomenon in which random transitions between states in a multistate system are modulated by an external periodic signal, is usually studied statistically. In an experiment with a period-doubled circuit, we observe transitions between the two phases of the response induced by noise or chaos. Adding a weak periodic modulation allows us to observe stochastic resonance. It is also noted that transitions between phases are caused by a crisis which may be observed in the circuit. As a result, we are able to describe stochastic resonance with the techniques of deterministic dynamics, providing a link between the fields of deterministic and stochastic mechanics.

PACS number(s): 05.20.−y, 05.45.+b

I. INTRODUCTION

The concept of stochastic resonance has recently been applied to such varied phenomena as the spectrum of nerve signals in hearing, the onset of the ice ages, and the detection of weak periodic signals buried in noise [1–3]. In the typical stochastic resonance situation, a sum of a noise signal and a weak periodic signal is used to drive a bistable system. By itself, the noise would cause the bistable system to make transitions randomly between the two states. If the amplitude of the noise signal is near the minimum amplitude required for the system to make transitions, then the probability of making a transition increases nonlinearly as the periodic signal strength increases. If one then filters the resulting signal with a two-state filter that only describes which state the system is in, the periodic component of the signal is greatly amplified.

This phenomenon has been shown to be ubiquitous in two-state systems, both in theory and in experiment [1–3]. The theory describing stochastic resonance is statistical; the noise is assumed to be white noise, and the probability of transition is derived from the laws of statistical mechanics [2,3]. The resulting probability depends exponentially on the noise strength.

We would like to show that it is also possible to view stochastic resonance from a dynamical systems viewpoint. We have written a preliminary account of our experiments [4]. It has been shown that stochastic resonance still occurs when chaos, rather than noise, is used as the nonperiodic component of the driving signal [5]. Chaos is a deterministic dynamical signal, so when chaos is used in place of noise for stochastic resonance experiments, the motion of the system is not predictable, but it is not random; the entire system is deterministic. This means that the "stochastic" resonance may be described using dynamical, rather than statistical, concepts.

We show in an experiment that stochastic resonance may be described in the same way as a crisis [6,7]. A crisis is a situation in which the stable manifold of an unstable periodic orbit collides with the unstable manifold of the same or a different periodic orbit. The stable manifold forms the boundary between different basins of attraction. The result is that one attractor collides with the basin of attraction of another, so that the two separate attractors become one. Using this description allows one to consider stochastic resonance as a particular case of a much larger group of dynamical phenomena, and to describe stochastic resonance through the use of dynamical concepts. There is other work describing stochastic resonance near a crisis, but the process itself is still considered statistically in that work [8,9]. Nicolis, Nicolis, and McKernan [10] have studied stochastic resonance in a chaotic two-well Duffing oscillator, where chaos provides the equivalent of the noise signal. Our work is different in that we consider a periodic one-well Duffing system where the chaos is added to the driving term. We also show that the behavior near the crisis may be modeled using dynamical concepts.

There is also a recent paper by King and Gaito [11] that uses a stochastic analogy to study a catastrophe in a deterministic two-well system. They use this analogy to understand the effect of changing the symmetry of the two wells on the dynamics of the system. Arrechi and co-workers have described the spectra produced by noise-induced hopping between different attractors in multistable systems [12,13]. Our work is also related to both research on noise-induced crises [14] and work on quasiperiodically driven Duffing systems [15].

II. EXPERIMENT

A. Period doubling

The experiment is based on a driven circuit simulating the single-well Duffing equations. This circuit has been described in previous work [16]. The circuit is described by the equations

$$\frac{dy}{dt}=\alpha[\,A\cos(\omega_d t)+\epsilon\cos(\omega_m t)+\eta f(t) + C-0.2y-G(x)]\,, \tag{1}$$

$$\frac{dx}{dt}=\alpha y\,, \tag{2}$$

$$G(x)=\begin{cases}0\ , & \text{abs}(x)<1.2\ ,\\ x-1.2\,\text{sgn}(x)\ , & 1.2\le\text{abs}(x)<2.6\ ,\\ 2x-3.8\text{sgn}(x)\ , & 2.6\le\text{abs}(x)\ ,\end{cases} \tag{3}$$

where A is the amplitude of the cosine drive and C is a constant offset that may be added to the drive. The frequency ω_d is the frequency of the periodic drive, and ω_m is the frequency of a small periodic modulation with amplitude ϵ. The function $f(t)$ may be either noise or chaos, and its amplitude is multiplied by η. The function $G(x)$ is a piecewise linear approximation to a cubic function. This function was used because it was much easier to characterize and match than other types of nonlinear functions available in circuits. The time factor α is $1\times10^4\ \text{s}^{-1}$.

The circuit is driven so that its response is period doubled. When period doubled, the response has two possible phases, one shifted by one drive cycle from the other. Figure 1 is a two-dimensional plot of a period-doubled attractor plotted from data from this circuit. It is possible to make the system shift from one phase to the other by adding noise or chaos to the drive signal. As we have shown previously, this phase flip occurs when the perturbed period-doubled circuit finds itself on an unstable period-1 orbit [16]. The period-1 orbit persists for one or more cycles, allowing the phase flip to occur. Because we are looking at two different phases as our two states, their symmetry is not affected by inaccuracies in the construction of the circuit.

The Duffing circuit is driven by a 726-Hz sine-wave signal with an rms amplitude of 4.6 V and an offset of 0.3 V from a signal generator. To this may be added a signal from a chaotic circuit or noise from a noise generator. A second function generator supplies a sinusoidal modulation signal that is also added to the drive. The drive signal generator also provides a synchronous signal, which is used to strobe a digitizer in order to collect a time series consisting of the output of the circuit at a constant phase of the drive. This time series is downloaded to a computer, where the data is used to determine the phase of the response.

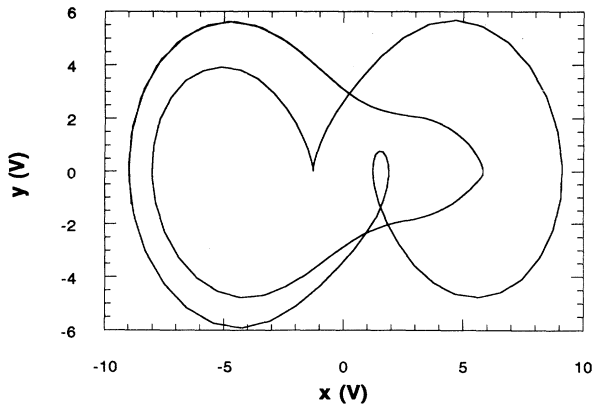

FIG. 1. Plot of the period-doubled attractor from the circuit used in these experiments.

The time series from the digitizer consists of a zigzag line of points. For most phases of the drive, such as the positive-going zero crossing, the unstable period-1 orbit that forms the boundary between the two phases will be approximately halfway between the two halves of the period-2 orbit, so the center line of the zigzag time series corresponds approximately to this unstable period-1 orbit. The phase variable is initially set to an arbitrary value, either 0 or 1. If the time series is above the center line at every even number of drive cycles and below at every odd number, the phase variable is set to 1. The opposite phase is set to zero. The initialization of the phase variable may produce a spurious indication of a phase flip at the beginning of the time series.

After 4096 cycles, the power spectrum of the phase time series is calculated. This is repeated for 20 time series and the resulting power spectra are averaged together.

To compare the effect of our deterministic chaos to that of noise, we used a chaotic signal from a hysteretic oscillator circuit [17] and white noise from a noise generator. Figure 2(a) shows the power spectrum of the chaotic signal, while Fig. 2(b) shows the spectrum of the noise. The amplitude distributions of both signals are shown in Fig. 3.

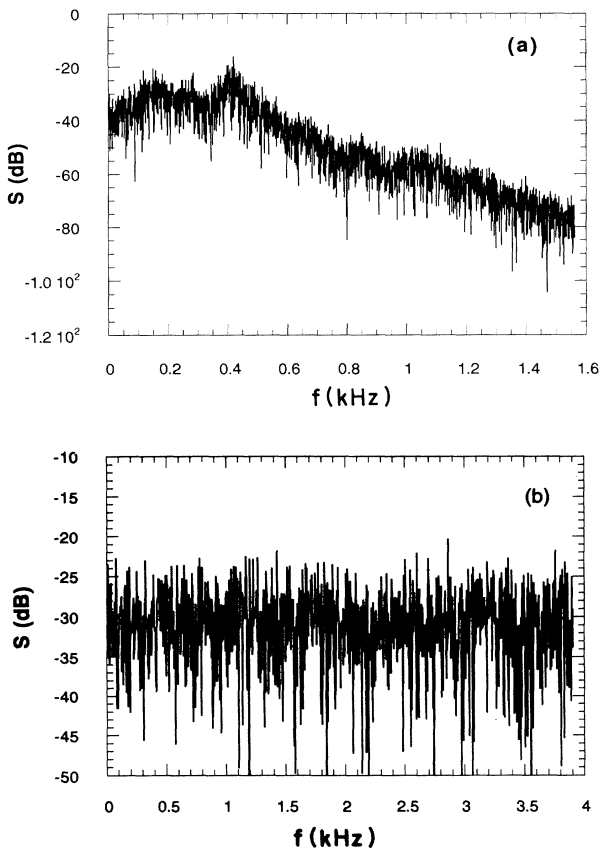

FIG. 2. (a) Power spectrum of chaos from a hysteretic oscillator circuit used in these experiments. (b) Power spectrum of noise from the noise generator used in these experiments.

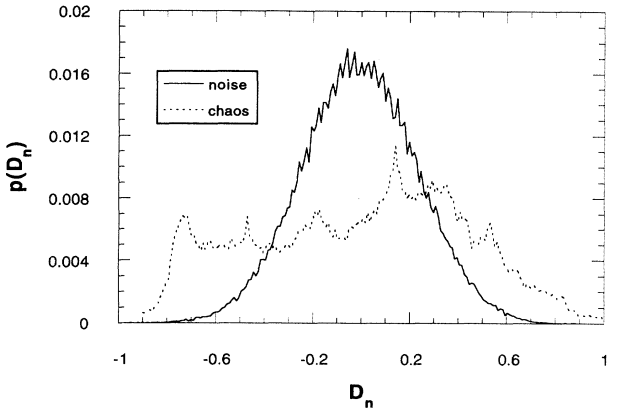

FIG. 3. Normalized distribution $p(D_n)$ of normalized amplitudes D_n of the signals from the noise generator (solid line) and the chaotic circuit (dotted line).

B. Crises

The experiment was first done with no modulation signal. The amplitude of the chaos added to the drive signal was first set to a low value, so that the period-doubled system did not flip phase. The amplitude of the chaos was then increased so that flipping did occur, and the average number of cycles between flips was recorded. The average cycles per flip versus chaos or noise amplitude is plotted in Fig. 4(a). This situation resembles crisis-induced intermittency [6,7].

Grebogi and co-workers [6,7] determined that the scaling of the number of transitions between different parts of the attractor after a crisis followed a power law of the form $K/(A-A_c)^{\gamma}$, where A in our experiment is the drive amplitude, A_c is the amplitude at which the crisis occurs, and γ is the exponent. It has been shown in experiments that this law also holds for noise-induced crises [14]. If we fit a power law of the form

$$K_1+\frac{K_2}{(A-A_c)^{\gamma}} \tag{4}$$

to the data in Fig. 4, we find that K_1 is -93, K_2 is 1967, A_c is 166 mV, and γ is 0.68 for chaos, and $K_1=-119$, $K_2=8211$, $A_c=213$ mV, and $\gamma=0.83$ for the noise. The additive constant K_1 is used to allow for the fact that our algorithm for finding phase flips may report up to 20 spurious flips due to initialization at the beginning of each time series.

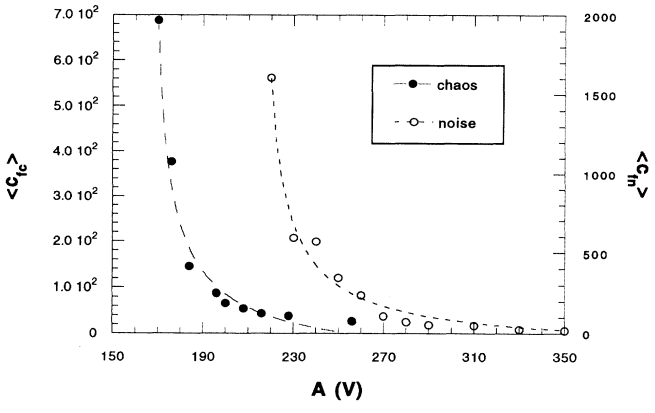

FIG. 4. Average number of cycles between phase flips for the period-doubled circuit when noise or chaos of rms amplitude A is added to the drive signal. On the left axis is the average number of cycles per flip $\langle c_{f_c} \rangle$ when chaos is used. On the right axis is the average number of flips $\langle c_{f_n} \rangle$ when noise is used. The dotted lines are fits to the type of power law in Eq. (4).

We use the periodically driven Duffing circuit dynamics as an approximation to the dynamics of the same circuit when noise or chaos is added to the drive. We have shown before [16] that if the added signal is not too large and the system is stable to the new driving, the dynamics are not greatly changed.

We would like to apply the theory of crises, which applies to deterministic dynamical systems, to the Duffing circuit. Since both the periodic drive signal and the chaos come from deterministic dynamical systems, their sum must also be the output of a dynamical system, so that when chaos is added to the drive, the Duffing circuit is still a deterministic dynamical system that is not very different from the original dynamical system. We also find below that the same theory gives good results when noise is added to the drive.

The factor by which the chaotic signal is multiplied before being added to the periodic signal is a parameter of the system. The theory of critical exponents for crises is not parameter specific; rather, it says that given a dynamical system, the critical exponent near a crisis depends only on the orbits involved in the crisis and not on which parameter is being changed. As long as the dynamical system fits the approximations in Ref. [7], namely that the tangency is approximately quadratic, then one may calculate the critical exponent for this crisis from the eigenvalues of the crisis-mediating periodic orbit, in our case an unstable period-1 orbit.

To apply the theory of crises, it is necessary to determine what type of crisis is present here. Grebogi *et al.* [7] show that the critical exponent for a crisis is determined by the eigenvalues of the unstable periodic orbit whose stable manifold forms the boundary between the basins of attraction of the stable orbits. We know from experiments that this unstable orbit is a period-1 orbit. The exponent will also depend on whether the crisis occurs when the stable manifold of the unstable periodic orbit becomes tangent to the unstable manifold of itself (a homoclinic tangency), or a different unstable orbit (a heteroclinic tangency).

To apply this theory, it is necessary to find the point on the attractor where the crisis first occurs. This was determined from digitized time series. For a given drive phase, the time series from the circuit without noise or chaos may have one of two phases. The phase was determined by finding the average value of the time series for a given drive phase and using this value as a midpoint. Which phase the circuit was in depended on which side

of the midpoint the time series was on.

Noise or chaos was then added to the periodic signal driving the circuit, causing the circuit to flip phase. For a noise amplitude just above the crisis, the value of the x and y variables in the circuit when the phase flipped were recorded. Figure 5 shows these locations as large dots superimposed on the attractor. As Fig. 5 shows, there are two locations where the crisis occurs. Both locations correspond to the same phase of the drive (1.2 V going negative) but opposite phases of the response.

Also shown as a dotted line in Fig. 5 is the unstable period-1 orbit. Recent developments in theory and experiment have shown how to stabilize unstable periodic orbits in chaotic systems using small perturbations to a parameter [18]. Other work has extended these methods so that unstable orbits may be tracked outside of the chaotic region [19]. This tracking method was applied to find the unstable period-1 orbit for the same parameter settings as the period-2 orbit.

The same tracking method can be used to locate the stable manifold of the unstable period-1 point for the drive phase at which the crisis first occurs. A computer with two digital-to-analog converters was used to set 40 000 different initial conditions for the circuit. A new initial condition was set when the drive signal passed through the phase for the first crisis, i.e., when the amplitude of the drive signal was 1.2 V and decreasing. The control that stabilized the unstable period-1 orbit was left on while these initial conditions were being set. After 100 cycles, the phase of the circuit was determined. The possibilities were period-2 phase A, period-2 phase B, or period-1 orbit. Figure 6 is a plot of the final state for each of 40 000 initial conditions. The black regions correspond to a final state of period-doubled phase A, the gray regions to period-doubled phase B, and the white to period-1 orbit. The period-1 orbit itself is unstable, so the white regions correspond to initial conditions that come within a window in the x coordinate of 0.3 V centered on the unstable period-1 point, and then are kept near the period-1 orbit by the controller. The white regions include portions of the stable manifold of the unstable period-1 point. The control used in this experiment does not greatly change the dynamics; it is used to keep the circuit near the period-1 orbit long enough so that it is easy to determine that it did come close to the period-1 point.

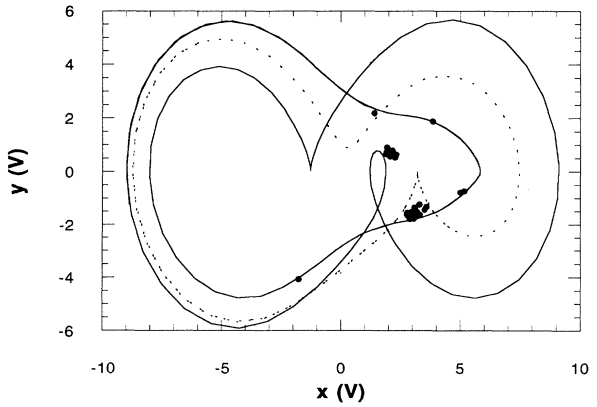

FIG. 5. Dots show the x and y coordinates where a phase flip occurs for a chaos or noise amplitude just above the crisis value. The solid line is the period-2 attractor, while the dotted line is the unstable period-1 orbit.

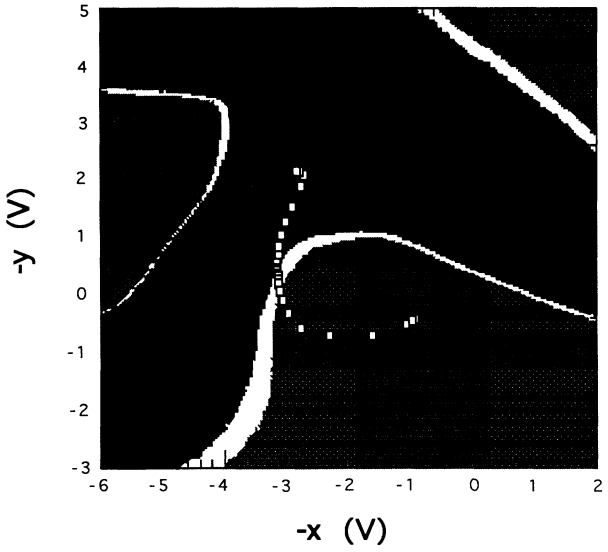

FIG. 6. Basins of attraction for the period-doubled circuit and unstable manifold for the unstable period-1 fixed point (all determined experimentally). The black corresponds to phase A of the period-2 orbit, the gray to phase B, and the white to the unstable period-1 orbit. The squares are a Poincaré section taken after setting the circuit to the unstable period-1 point and watching it move to the period-2 points. The axes are labeled $-x$ and $-y$ because the directions are reversed by the setup used to set the initial conditions.

The squares superimposed on Fig. 6 follow along the unstable manifold. With no control on, the digital-to-analog converters were used to set an initial condition very close to the unstable period-1 point. The output of the circuit was then strobed every time the drive passed through the phase for the first crisis. The output from the circuit moves away from the period-1 point along the unstable manifold until it comes to the two period-2 points.

The output of the circuit when noise or chaos is added to the periodic drive may be strobed at the same drive phase used to plot the manifolds to generate pseudo-Poincaré sections of the system. We call these pseudo-Poincaré sections because we use only the periodic part of the drive to generate them. Figure 7 shows such a section when the noise level is below that required for a crisis. The period-1 point is shown as a black dot. The two period-2 points have become large fuzzy regions stretching out along the unstable manifold of the period-1 point. The crisis occurs when these regions touch the stable manifold of the period-1 point. This crisis involves the stable and unstable manifolds of the same period-1 point, making it a homoclinic crisis.

Grebogi *et al.* [7] show that for a crisis caused by a homoclinic tangency in a two-dimensional system, the

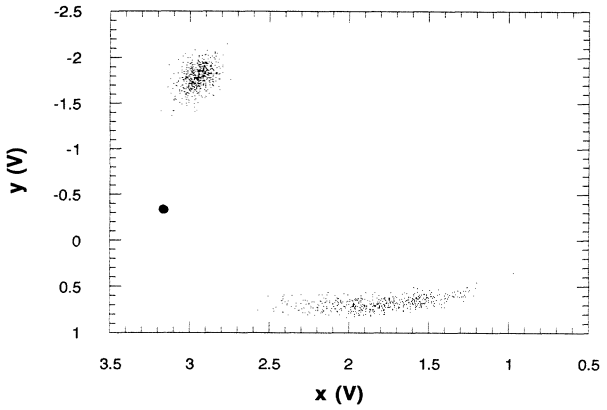

FIG. 7. Poincaré section of the Duffing circuit when noise has been added to the periodic drive. The large dot is the location of the unstable period-1 point.

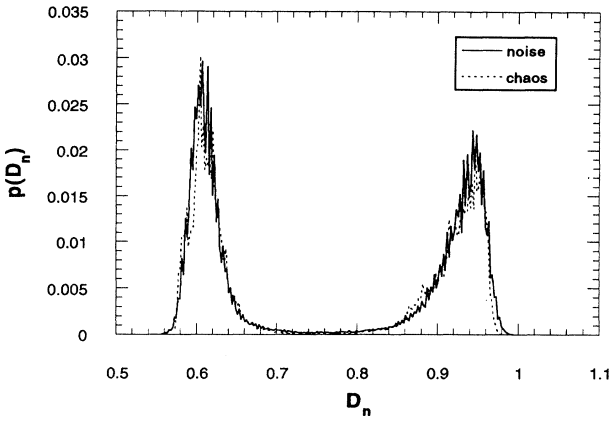

FIG. 8. Amplitude distributions $p(D_n)$ of the normalized amplitude D_n of the x signal from the period-doubled Duffing circuit for a constant phase of the drive. The solid line corresponds to the noise, while the dotted line corresponds to the chaos.

value of the exponent γ is given by

$$\gamma=\frac{\ln|\beta_2|}{\ln|\beta_1\beta_2|^2}\ , \tag{5}$$

where β_1 and β_2 are the unstable and stable eigenvalues of the orbit involved in the crisis. To find these eigenvalues, the circuit was started at ten slightly different initial conditions near the unstable period-1 point. The three components of the initial conditions were recorded by a digitizer, as were the three corresponding values 20 μs (about 1/75th cycle) later. The method of Eckmann *et al.* [20] was then used with the experimental data to find the eigenvalues for the unstable point. The magnitudes of the three eigenvalues were 1.14, 0.65, and 0.0002. The dynamics were approximately two dimensional here, so Eq. (2) may be used. The resulting value of γ was 0.72, close to the value measured from the power-law fit of 0.68 for chaos and 0.83 for noise. This supports the claim that the flipping of the phases occurs due to a crisis. This is not surprising when chaos is used, for the entire system is then deterministic. It is more surprising when noise is used, as the noise signal was not deterministic.

The fact that we see a crisis when noise is used is a consequence of the fact that the noise is driving a deterministic system. The noise distribution itself, as pictured in Fig. 3, has an exponential tail, so that we would expect the number of phase flips to increase exponentially as the noise amplitude increases. This is not the case because the Duffing circuit is not being driven adiabatically by the noise. Rather, the circuit acts as a bandpass filter; noise frequencies near the center of the pass band will have a much larger effect on the circuit than frequencies far from the center. In Fig. 8 is plotted the actual amplitude distribution of the driven period-doubled Duffing circuit strobed with the maximum of the sinusoidal drive signal. It may be seen that the distributions for the chaos and the noise are almost the same. Least-squares fits confirm that, except for an exponential tail for very small probabilities, the distribution for the noisy Duffing circuit follows almost the same power law (with an exponent of approximately 3) as the chaotic driven Duffing circuit. The half-width at half-maximum of the amplitude distribution for the driven period-doubled circuit also obeys a power law as the noise amplitude is increased, with an exponent of approximately 1.6.

C. Stochastic resonance

For our stochastic resonance studies, we added a small periodic signal (the modulation signal) to the drive. We used a 100-Hz sine wave with an amplitude of 180 mV rms or a 300-Hz sine wave of 72 mV rms. The 100-Hz signal was larger than the 300-Hz signal because the circuit acts as a bandpass filter. Frequencies farther from the center of the band (which was near 700 Hz) had a smaller effect on the circuit than those closer to the center.

The periodic modulation shifts the location of the unstable period-1 point and the period-2 points. Figure 9 shows a pseudo-Poincaré section of the two period-2

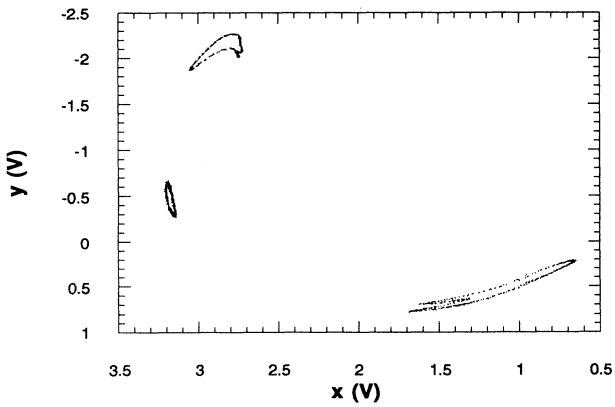

FIG. 9. Poincaré sections of the period-doubled Duffing circuit and the controlled unstable period-1 orbit of the Duffing circuit when a 300-Hz modulation has been added to the drive.

points and the controlled unstable period-1 point when a 300-Hz modulation signal was added to the drive. The movement of the period-1 point in a periodic fashion causes the noise amplitude for a crisis to behave periodically. This is similar to the modulation of a potential barrier in stochastic resonance. If noise or chaos is added to the drive signal at the same time as the modulation, stochastic resonance does occur.

Figure 10 is a power spectrum of the phase time series for a modulation frequency of 100 Hz when the chaos amplitude was 64 mV rms. The spectrum shows a peak at the modulation frequency and two odd subharmonics at 25 and 75 Hz, and a peak at 265 Hz. This last peak corresponds to the difference between half the driving frequency (726 Hz) and the modulation frequency (100 Hz). Because we take our data at the drive frequency, the spectrum only goes up to half the drive frequency. The background spectrum is not Lorentzian, as is typical of stochastic resonance [1–3], because the adiabatic approximation does not hold here.

Figure 11 shows the signal-to-noise ratios of the peaks at 100 and 265 Hz as the amplitude of the chaos is increased. The signal-to-noise ratio was found by comparing the amplitude of a peak to the amplitude of the background power spectrum within 5 Hz on either side of the peak, as is standard in stochastic resonance. The noise value is an average of the nearby noise background, and we estimate to be within ± 0.5 dB of the noise at the location of the peak. The signal-to-noise ratio at 100 Hz drops linearly with the chaos amplitude, indicating no stochastic resonance, while at 265 Hz, the signal-to-noise ratio increases at first as the chaos amplitude increases, indicating stochastic resonance. The reason that we see stochastic resonance at 265 Hz and not at the fundamental is because we are using a period-doubled system.

It was shown above that just above the crisis, there is one phase of the drive for which the circuit can flip phase. Well above the crisis, there are more points, but one point is still more likely than the others. The transition probability is therefore modulated by the drive frequency f_d. The probability of flipping is also larger when

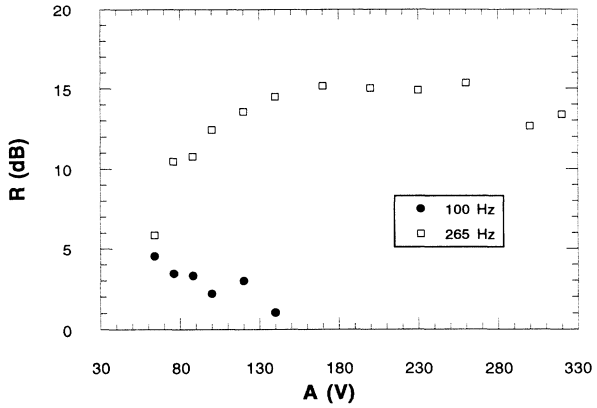

FIG. 11. Signal-to-noise ratio R vs chaos amplitude A for spectral lines at 100 and 265 Hz when a 100-Hz modulation and chaos are added to the drive for the period-doubled Duffing circuit.

the modulation signal is at a maximum, so this rate should be proportional to f_m, where f_m is the modulation frequency. These two rates are not independent; i.e., if the system is at the point on the attractor where flips are most likely to occur but the modulation is at a minimum, flipping is very unlikely. One rate will modulate the other, so the actual rate is proportional to the product of periodic functions, like $\sin(f_m)\times\sin(f_d)$. From the identity $\sin(\alpha)\sin(\beta)=\frac{1}{2}\cos(\alpha-\beta)-\frac{1}{2}\cos(\alpha+\beta)$, the sum and difference frequencies will be present. Because the circuit is nonlinear, harmonics of these frequencies are also present. Because the time series is digitized at f_d, the largest frequency in the output spectrum is $f_d/2$, and the largest modulation term that is visible is $f_d/2-f_m$.

Figure 12 shows the power spectrum of the phase time series when the modulation frequency is a 300-Hz sine wave with an amplitude of 72 mV rms. The modulation at 300 Hz is visible along with $f_d/2-f_m$ at 68 Hz, and several other subharmonics that are not amplified. In

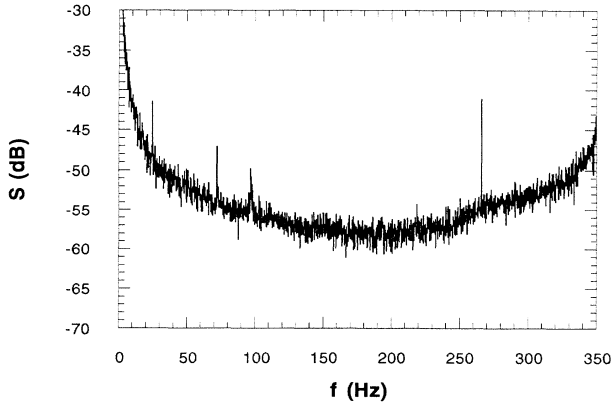

FIG. 10. Power spectrum of the phase time series for the period-doubled Duffing circuit when chaos and a 100-Hz modulation have been added to the drive.

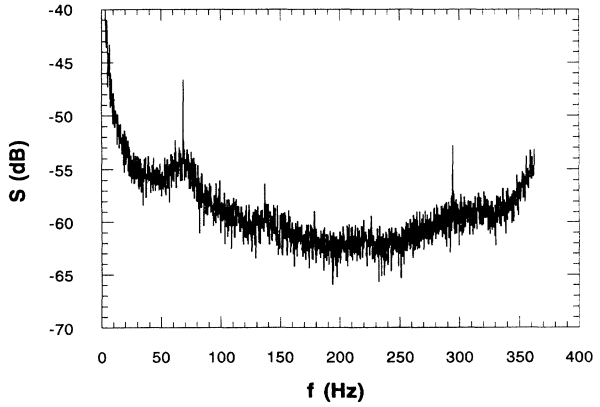

FIG. 12. Power spectrum of the phase time series for the period-doubled Duffing circuit when chaos and a 300-Hz modulation have been added to the drive.

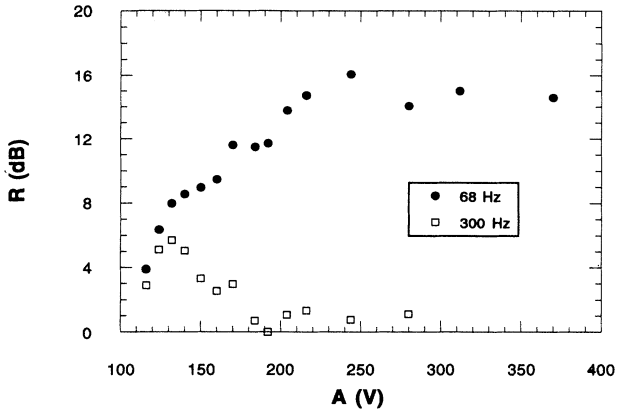

FIG. 13. Signal-to-noise ratio R vs chaos amplitude A for spectral lines at 68 and 300 Hz when a 300-Hz modulation and chaos are added to the drive for the period-doubled Duffing circuit.

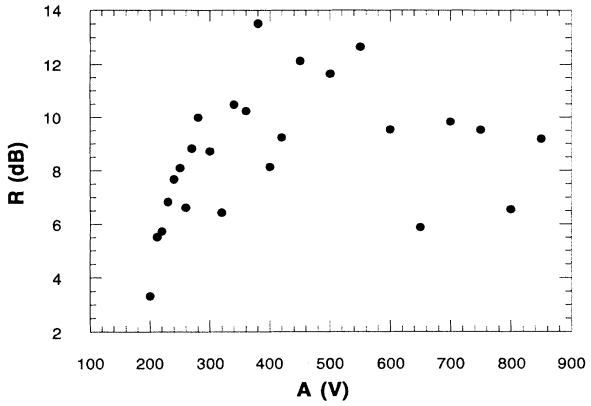

FIG. 15. Signal-to-noise ratio R vs noise amplitude A for the spectral line at 68 Hz when a 300-Hz modulation and noise have been added to the drive for the period-doubled Duffing circuit.

Fig. 13, one may again see that the main stochastic resonance effect takes place for the frequency $f_d/2-f_m$. There appears to be some small amplification of the modulation frequency for small amplitudes of chaos. It is not certain if this is real or due to measurement errors.

The more typical type of stochastic resonance involves noise instead of chaos. White noise from the noise generator was added to the drive signal when a 300-Hz modulation was present, producing the power spectrum seen in Fig. 14. The stochastic resonance effect was similar to that observed with chaos, although it was not as large. The signal-to-noise ratios for this spectrum are shown in Fig. 15. It was harder to determine which phase the circuit was in when larger amplitudes of noise were used, so the signal-to-noise ratio shows much scatter. The stochastic resonance effect here is not as large as when chaos is used, probably because the noise distribution is much more spread out, as was shown in Fig. 3. The chaos amplitude distribution increases much faster for large amplitudes, so the probability of phase flipping changes much more quickly as the chaos amplitude is increased when just above the crisis.

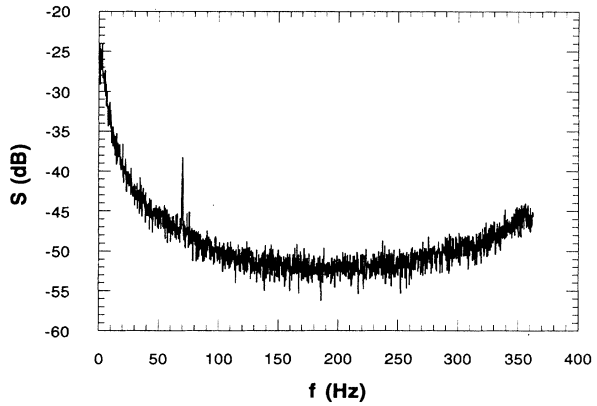

FIG. 14. Power spectrum of the phase time series for the period-doubled Duffing circuit when noise and a 300-Hz modulation have been added to the drive.

III. THEORY

The theory most commonly used in describing stochastic resonance was developed by McNamara and Wiesenfeld [2]. They look at a two-state system where the two states are designated by + and −. The probability that the system is in the ± state is $n_{\pm}$, while the rate of transition out of the ± state is $W_{\pm}$. The change in population of the + state is given by

$$\frac{dn_+}{dt}=W_-(t)-[W_+(t)+W_-(t)]n_+ \ . \tag{6}$$

McNamara and Wiesenfeld solve this equation and then, assuming a rate of the form

$$W_{\pm}(t)=f(\mu\pm\eta_0\cos\omega_m t) \ , \tag{7}$$

they derive the form of the power spectrum for this system.

To find a rate law for the period-doubled system, we start with the observation that in the unmodulated system, the average time between phase flips was given by a critical power law. This power-law form may be inverted to give a flipping rate for the crisis:

$$W_{\pm}(t)=\frac{(x-A_c)^{\gamma}}{K_2} \ , \tag{8}$$

where x is the chaos amplitude, A_c is the chaos amplitude at which the crisis occurs, and γ and K_2 come from Eq. (4). The additive constant in Eq. (4) is set equal to 0 because transitions out of a particular phase are not possible below the critical chaos amplitude. The constant was present in Eq. (4) because our algorithm for finding phase flips always gave a small number of flips, even when none were present.

Adding the modulation signal will change this rate. Figure 9 shows how this effect occurs. With the modula-

tion added to the drive, previously described control techniques based on the Ott-Grebogi-Yorke method [18] were used to keep the circuit in the unstable period-1 orbit that the system had to go through in order to flip phase. In Fig. 9 are plotted Poincaré sections of the modulated unstable period-1 orbit and the modulated stable period-2 orbit. The modulated period-1 orbit forms a torus, sometimes coming closer to one half of the period-2 orbit, sometimes coming closer to the other. The effect of this will be to change the critical chaos amplitude at which the period-2 orbit touches the stable manifold of the period-1 orbit, which is the boundary between the basins of attraction between the two period-2 states. To account for this, the rate law is changed to

$$W_{\pm}(t)=\frac{(x-A_c\pm\eta_m\cos\omega_m t)^{\gamma}}{K_2}\ , \tag{9}$$

where η_m is the modulation amplitude and ω_m is the modulation frequency. No transitions are possible if the attractors do not overlap, so when the numerator is less than or equal to 0, $W_{\pm}(t)$ is set equal to 0. This rate is in the same form as Eq. (4), with $(x-A_c)$ corresponding to μ. McNamara and Wiesenfeld [2] actually work out a simple example that corresponds to our rate law with a critical exponent of $\gamma=1$.

Equation (6) was numerically integrated with the rate law of Eq. (9), using a fourth-order Runge-Kutta integration routine and a modulation frequency ω_m of 100 Hz. The autocorrelation function and power spectrum were found using methods similar to those used in McNamara and Wiesenfeld. The resulting power spectra showed peaks at the modulation frequency and odd harmonics, as may be seen in Fig. 16. Stochastic resonance effects were seen as the amplitude of the chaos or noise was increased. The signal-to-noise ratio at the modulation frequency is plotted in Fig. 17.

Using a crisis-rate law such as that in Eq. (9) also allows the prediction of other characteristics of the stochastic resonance. It was seen numerically, for example, that the peak signal-to-noise ratio during stochastic resonance increased exponentially as γ increased.

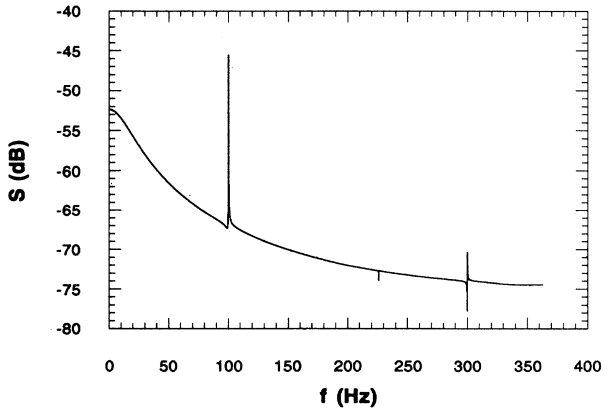

FIG. 16. Numerically generated power spectrum found by using the rate law of Eq. (9) with the McNamara and Wiesenfeld theory. The modulation frequency was 100 Hz.

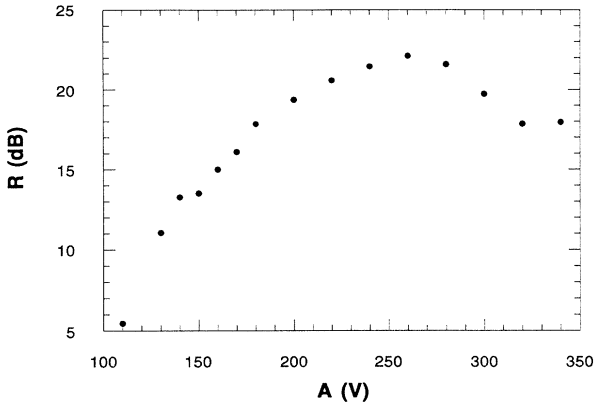

FIG. 17. Numerically generated signal-to-noise ratio R vs noise amplitude A for the spectral line at 100 Hz found by using the rate law of Eq. (9) with the McNamara and Wiesenfeld theory.

It was also possible to predict the location of the peak signal-to-noise ratio using the crisis approach. When the amplitude of the chaos was low or moderate, the modulation term in Eq. (9) sometimes caused the rate to be positive and finite, and sometimes zero. When the chaos amplitude x was greater than $A_c+\eta_m$, the rate was always positive. Because of this, the effect of the modulation was not as large when the chaos amplitude reached this point. The signal-to-noise ratio should not increase above this point, designated as $X_{\max}$. For 100-Hz modulation of the period-doubled orbit, $A_c+\eta_m$ is 238 mV. From Fig. 17 (numerical result) and Fig. 11 (experimental result), it may be seen that the signal-to-noise ratio begins to decrease when the chaos amplitude is near this value. For the 300-Hz modulation in Fig. 13, $A_c+\eta_m$ is 238 mV, which is also the chaos or noise amplitude for the maximum signal-to-noise ratio. When noise is added to the drive, the maximum signal-to-noise ratio in Fig. 15 should be near 285 mV. Because of the difficulty in determining which phase the system is in for high levels of noise, it is hard to tell if this rule is obeyed in this case.

IV. CONCLUSIONS

Stochastic resonance, a subject that is usually studied statistically, may also be studied using techniques developed to study deterministic systems. We have shown in a period-doubled Duffing circuit that stochastic resonance effects may be caused by a deterministic crisis. This crisis is very similar when deterministic chaos or white noise is used. These different cases are similar because the noise is affected by the deterministic dynamics of the Duffing circuit, as was shown in Figs. 7 and 8.

This work suggests that adding chaos or noise to a dynamical system does not just "mess up" the system. There are measurable dynamical effects that take place. This is especially important if one considers the driving of dynamical systems with chaos. In this case, this paper shows that since the resulting dynamical system is completely deterministic, the techniques of deterministic dy-

namics are appropriate to describe the behavior of the system. It is also shown that the same deterministic techniques worked when random noise was used to drive the system.

ACKNOWLEDGMENT

The authors acknowledge useful conversations with Celso Grebogi, Ed Ott, Jim Heagy, and Steve Hammel.

[1] F. Moss (unpublished).
[2] B. McNamara and K. Wiesenfeld, Phys. Rev. A **39**, 4854 (1989).
[3] P. Jung and P. Hanggi, Phys. Rev. A **41**, 2977 (1990).
[4] T. L. Carroll and L. M. Pecora, Phys. Rev. Lett. **70**, 576 (1993).
[5] E. Ippen, J. Lindner, and W. Ditto, J. Stat. Phys. **70**, 437 (1993).
[6] C. Grebogi, E. Ott, and J. A. Yorke, Physica D **7**, 181 (1983).
[7] C. Grebogi, E. Ott, F. Romeiras, and J. A. Yorke, Phys. Rev. A **36**, 5365 (1987).
[8] V. S. Anishchenko, M. A. Safonova, and L. O. Chua, Int. J. Bifurcations Chaos **2**, 397 (1992).
[9] V. S. Anishchenko, A. B. Neiman, and M. A. Safanova, J. Stat. Phys. **70**, 183 (1993).
[10] G. Nicolis, C. Nicolis, and D. McKernan, J. Stat. Phys. **70**, 125 (1993).
[11] G. P. King and S. T. Gaito, Phys. Rev. A **46**, 3092 (1992).
[12] F. T. Arrechi, R. Badii, and A. Politi, Phys. Rev. A **32**, 402 (1985).
[13] F. T. Arrechi and A. Califano, Europhys. Lett. **3**, 5 (1987).
[14] J. C. Sommerer, W. L. Ditto, C. Grebogi, E. Ott, and M. L. Spano, Phys. Rev. Lett. **15**, 1947 (1991).
[15] J. F. Heagy and W. Ditto, J. Nonlin. Sci. **1**, 423 (1991).
[16] T. L. Carroll and L. M. Pecora (unpublished).
[17] T. L. Carroll and L. M. Pecora, IEEE Trans. Circuits Syst. **38**, 453 (1991).
[18] E. Ott, C. Grebogi, and J. A. Yorke, Phys. Rev. Lett. **64**, 1196 (1990); W. L. Ditto, S. N. Rauseo, and M. L. Spano, *ibid.* **65**, 1947 (1990); E. R. Hunt, *ibid.* **67**, 1953 (1991).
[19] T. L. Carroll, I. Triandaf, I. Schwartz, and L. Pecora, Phys. Rev. A **46**, 6189 (1992).
[20] J.-P. Eckmann, S. Ollifson Kamphorst, D. Ruelle, and S. Ciliberto, Phys. Rev. A **34**, 4971 (1986).

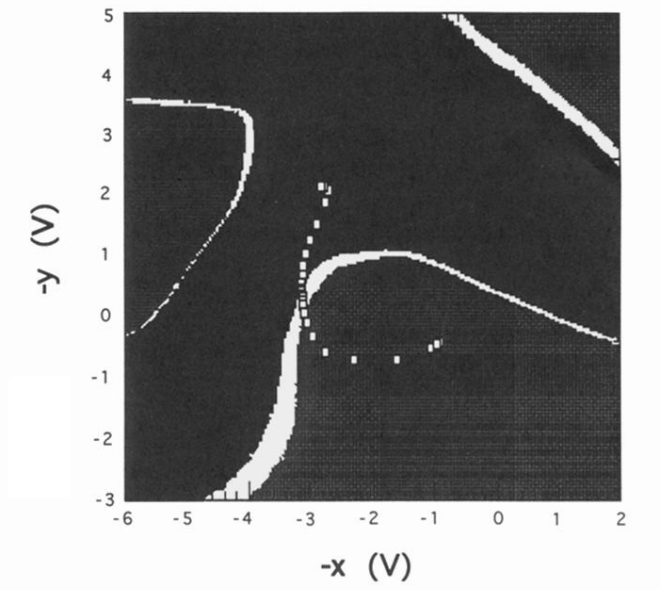

FIG. 6. Basins of attraction for the period-doubled circuit and unstable manifold for the unstable period-1 fixed point (all determined experimentally). The black corresponds to phase A of the period-2 orbit, the gray to phase B, and the white to the unstable period-1 orbit. The squares are a Poincaré section taken after setting the circuit to the unstable period-1 point and watching it move to the period-2 points. The axes are labeled $-x$ and $-y$ because the directions are reversed by the setup used to set the initial conditions.